Epitaxial growth and magnetic properties of half-metallic Fe$_3$O$_4$ on GaAs(100)

Y. X. Lu, J. S. Claydon, and Y. B. Xu*

Spintronics Laboratory, Department of Electronics, The University of York, York, YO10 5DD, United Kingdom

S. M. Thompson

Department of Physics, The University of York, York, YO10 5DD, United Kingdom

K. Wilson

Department of Chemistry, The University of York, York, YO10 5DD, United Kingdom

G. van der Laan

CCLRC Daresbury Laboratory, Warrington WA4 4AD, United Kingdom

The growth and magnetic properties of epitaxial magnetite Fe$_3$O$_4$ on GaAs(100) have been studied by reflection high-energy electron diffraction, x-ray photoelectron spectroscopy, magneto-optical Kerr effect, and x-ray magnetic circular dichroism. The epitaxial Fe$_3$O$_4$ films were synthesized by *in situ* post growth annealing of ultrathin epitaxial Fe films at 500 K in an oxygen partial pressure of 5×10^{-5} mbar. The XMCD measurements show characteristic contributions from different sites of the ferrimagnetic magnetite unit cell, namely, Fe$_{td}^{3+}$, Fe$_{oh}^{2+}$, and Fe$_{oh}^{3+}$. The epitaxial relationship was found to be Fe$_3$O$_4$(100)⟨011⟩//GaAs(100)⟨010⟩ with the unit cell of Fe$_3$O$_4$ rotated by 45° to match that of GaAs(100) substrate. The films show a uniaxial magnetic anisotropy in a thickness range of about 2.0–6.0 nm with the easy axes along the [0$\bar{1}$1] direction of the GaAs(100) substrate.

One of the major steps in developing next generation spintronic devices is the synthesis of magnetic/semiconductor hybrid materials with high efficient spin injection and the Curie temperature above room temperature.[1–4] Spin injection and detection using ferromagnetic transition metals such as Fe, Co, and Ni have been demonstrated, but the efficiency is less than 1–2 % apart from the large effect observed in photoexcitation and photoemission experiments with circularly polarized light.[5,6] On the other hand, based on easy integration with semiconductor substrate, the III-V based diluted magnetic semiconductors (DMS's) have been proposed as promising candidates but their Curie temperatures are well below room temperature so far.[7–9] At the same time, half-metallic Fe$_3$O$_4$, called magnetite, has attracted great attention recently for spintronics as it has high polarization at the Fermi level[10] and relatively high electronic conductivity at room temperature,[11] which is believed to benefit the injection of spin carriers into the semiconductors. Epitaxial growth of Fe$_3$O$_4$ on MgO,[12–14] Al$_2$O$_3$,[13] and Pt (Ref. 15) has been demonstrated by several groups and several interesting magnetic properties such as superparamagnetism,[12] slow saturation behavior,[13] and local out-of-plane magnetic moments in zero field[13] have been observed. However, in order to incorporate Fe$_3$O$_4$ into spintronics devices, synthesis of Fe$_3$O$_4$ on semiconductor substrates, such as GaAs, might be essential. In this Brief Report, we present the growth and the magnetic properties of epitaxial ultrathin Fe$_3$O$_4$ films on GaAs(100). As far as we know, this might be the first time that a half-metallic iron oxide/semiconductor hybrid structure has been synthesized.

There are basically two approaches of synthesis of Fe$_3$O$_4$ reported in the literature.[10–16] The first approach is to deposit Fe on the substrate, then oxidize the epitaxial Fe with oxidizing agents such as O$_2$ and NO$_2$. The oxidation thickness of the Fe can be as thick as 56 Å for 1200 L (1 L $=1$ Langmuir$=1 \times 10^{-6}$ mbars) O$_2$ exposure.[16] Another growth procedure is to epitaxially grow Fe$_3$O$_4$ samples directly by oxidizing the evaporated Fe atoms in an oxygen rich environment.[13] We followed the first approach, growing epitaxial Fe films on GaAs substrates first and then oxidizing the films to form Fe$_3$O$_4$ in a UHV chamber. The undoped epiready GaAs(100) wafer was purchased from Wafer Technology, Ltd., with EJ Flat Option, i.e., the major flat is parallel to the [011] crystallographic direction. The substrate was chemically cleaned using an H$_2$SO$_4$:H$_2$O$_2$:H$_2$O (4:1:1) solution for 30 s, followed by deionized (DI) water rinsing and isopropyl alcohol (IPA) vapor cleaning. After being transferred into the UHV chamber, the substrate was annealed at 830 K for about 30 min until a sharp reflection high-energy electron diffraction (RHEED) pattern can be identified as shown in Fig. 1(a).

The Fe films were grown at a rate of approximately 2 Å/min, as monitored by a quartz microbalance, using an *e*-beam evaporator while the substrate temperature was held at room temperature. We would like to note that the nominal thicknesses of these predeposited Fe layers were quoted for the samples after oxidation. It has been shown that room-temperature growth could produce a ferromagnetic Fe film with a bulklike moment after the onset of the ferromagnetism, and the magnetic dead layer could be avoided by suppressing the formation of Fe-As nonmagnetic compounds at the interface.[17] Figure 1(b) is the RHEED pattern of a 6.0 nm Fe film grown on the GaAs (100) substrate, which confirms the epitaxial growth of Fe on GaAs (100). From the figure, we can know that the Fe film takes a bcc structure with the epitaxial relationship of
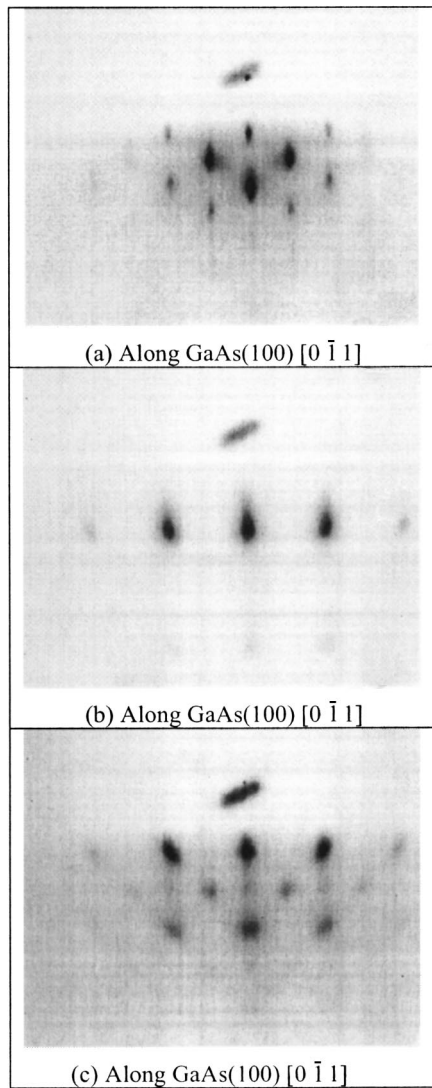
(a) Along GaAs(100) [0 $\bar{1}$ 1]

(b) Along GaAs(100) [0 $\bar{1}$ 1]

(c) Along GaAs(100) [0 $\bar{1}$ 1]

FIG. 1. RHEED patterns of (a) GaAs(100) substrate after cleaning and *in situ* annealing, (b) 6.0 nm of epitaxial Fe on GaAs(100), and (c) Fe_3O_4 formed by annealing at 500 K in an oxygen partial pressure. The electron beam was along the [0$\bar{1}$1] direction of the GaAs(100) substrate and the beam energy was set at 10.0 kV in the above diffraction.

FIG. 2. Fe $2p$ core-level XPS spectroscopy from the 6.0 nm (nominal) sample excited by Mg-K_α. The x-ray is perpendicular to the surface of the sample.

$Fe(100)\langle001\rangle//GaAs(100)\langle001\rangle$. This alignment is consistent with other groups' reports and our previous work.[17]

After iron growth the sample was exposed to O_2 in the growth chamber, maintaining the O_2 partial pressure at 5×10^{-5} mbar with a leak valve. The distance from the O_2 nozzle to the sample was around 12 cm. This would allow formation of a uniform pressure around the sample. Figure 1(c) shows the RHEED pattern of the sample after 3 min of oxidization at a substrate temperature of 500 K. No further change of RHEED patterns was observed with further annealing at the same environment, suggesting that the sample had reached a stable structure. This RHEED pattern is the same as that observed in epitaxial Fe_3O_4/MgO(100) (Ref. 14) with the incident electron beam along the [010] direction of Fe_3O_4, while in this work, the electron beam was along [0$\bar{1}$1] direction of the GaAs(100) substrate. This
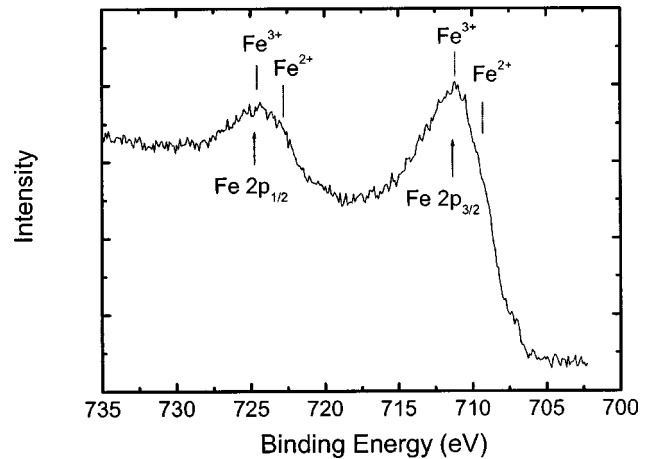
suggests that in our work the $\langle010\rangle$ directions of the epitaxial magnetite cell parallel the $\langle0\bar{1}1\rangle$ directions of the GaAs(100) substrate, with an epitaxial relationship of $Fe_3O_4(100)\langle011\rangle//GaAs(100)\langle010\rangle$.

As γ-Fe_2O_3 has a rather similar crystal structure to that of Fe_3O_4, the samples have been characterized using x-ray photoelectron spectroscopy (XPS). It is well established that the satellites in the XPS spectroscopy can help to identify the chemical states, for example, different chemical states of iron in its oxides.[18–20] One remarkable difference between the γ-Fe_2O_3 (maghemite) and the Fe_3O_4 (magnetite) is that the former has satellites in the Fe $2p$ core level spectra while the latter does not have. Figure 2 shows the Fe $2p$ core-level spectroscopy of the 6.0 nm sample, obtained with normal emission using Mg-K_α radiation, which agrees well with the Fe_3O_4 spectra reported.[18–20] The broad Fe $2p$ peaks are attributed to the coexistence of Fe^{3+} and Fe^{2+} states, and at the same time, that no satellite can be identified around the binding energy of 719.0 eV, excludes the possible presence of maghemite (γ-Fe_2O_3) in our samples. It is worthwhile to note that the XPS spectra along with the x-ray magnetic circular dichroism (XMCD) data in Fig. 5 show no sign of contribution from metallic Fe, indicating that these ultrathin Fe films were fully oxidized.

Figure 3 is a schematic diagram of the proposed alignment of the magnetite cell rotated by 45° relative to the GaAs (100) substrate. The rotation of 45° might be due to the fact that the $Fe_3O_4(100)\langle011\rangle$ directions, rather than $Fe_3O_4(100)\langle010\rangle$ directions, matches better with GaAs(100)$\langle010\rangle$ directions. The lattice constant of GaAs is 5.654 Å, and for Fe_3O_4, it is 8.396 Å. Simple calculation shows the mismatch between Fe_3O_4 and GaAs is around 5.0% if the Fe_3O_4 cell is rotated by 45° relative to GaAs cell in the (100) plane. This might be the reason that epitaxial magnetite can be stabilized on GaAs(100) as demonstrated here. However, we should note that although the relative rotation of the magnetite cells can be confirmed, it is not clear whether the Fe_3O_4 is rotated clockwise or anticlockwise relative to GaAs. The coherent Fe might be oxidized into one dominant rotated state due to the inverse spinel structure of the Fe_3O_4.
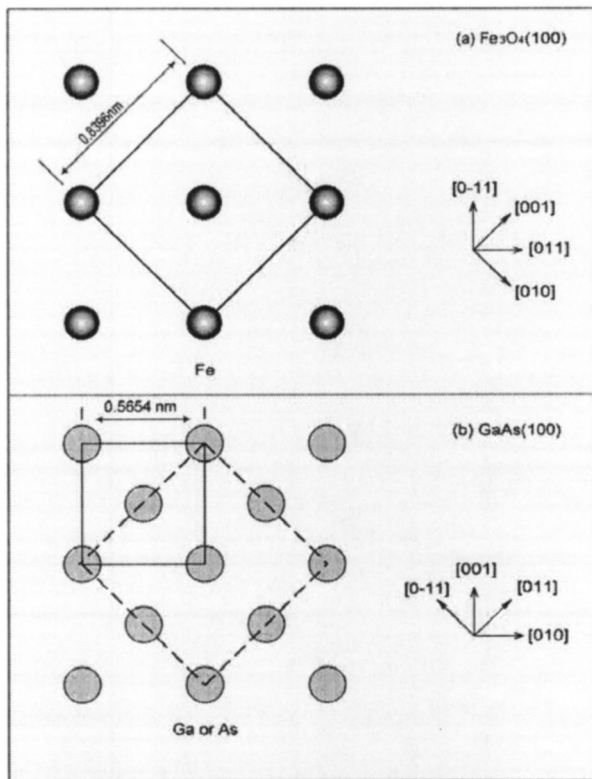
FIG. 3. Proposed epitaxial relation of (a) epitaxial Fe_3O_4 on (b) GaAs(100). The unit cells and the lattice distances have been indicated by solid lines. The Fe_3O_4 unit cell has been rotated by 45° in the plane of (100) relative to GaAs. The dash line in (b) indicates one possible unit accommodating one Fe_3O_4 unit cell. Note in (a) only Fe ions in the bottom layer of a unit cell have been shown. Insets show major axes of both materials.

The magnetic properties of the films were studied by *ex situ* magneto-optical kerr effect (MOKE) at room temperature using an electromagnet with a maximum field of 1.6 kOe and a stabilized diode laser with a 780 nm wavelength. The samples were transferred in the air without a capping layer since Fe_3O_4 is one of the most stable iron oxides and any capping layer might change the magnetic properties of the films. The configuration of the MOKE was transverse in which the applied magnetic field was in the plane of the films. No MOKE signal was detected with thickness less than 1.0 nm, suggesting the films may be nonmagnetic at room temperature at the initial stage. At a narrow thickness range of around 1.6 nm, S-shaped MOKE loops with zero hysteresis were observed suggesting that the films are superparamagnetic as that found in Fe/GaAs system.[17] The superparamagnetic behavior could be due to the formation of disconnected clusters, which are unable to stabilize a long-range ferromagnetic order at room temperature. The antiphase boundaries (APB's) among the clusters could also be responsible for this superparamagnetic behavior as suggested by Voogt *et al.*[12]

Magnetic uniaxial anisotropy was observed in a thickness range of about 2.0–6.0 nm as shown by Fig. 4 of the MOKE loops along their four major axes. At a thickness of 2.0 nm, a uniaxial magnetic anisotropy is clearly defined and around 4.2 nm, the system still exhibits a uniaxial anisotropy. While
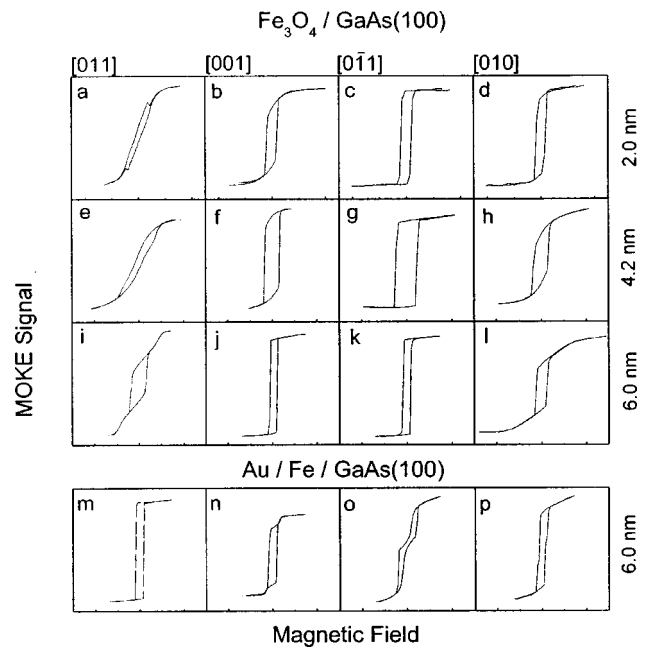

FIG. 4. MOKE loops of Fe_3O_4/GaAs(100) [up panel, (a)–(l)] and Au/Fe/GaAs(100) [bottom panel, (m)–(p)]. The nominal thicknesses of the samples are indicated to the right of the panels. The directions of the external magnetic field are labeled on top of each column according to the GaAs(100) substrate. Note the magnetic field in the first row (a)–(d) was $-0.25 - +0.25$ kOe, while in other rows (e)–(p), it was $-0.75 - +0.75$ kOe.

at the thickness of 6.0 nm, the cubic anisotropy of the bulk Fe_3O_4 presents and rotates the global easy axis slowly away from the $[0\bar{1}1]$ direction. The easy axis of this uniaxial magnetic anisotropy (UMA) is along the $[0\bar{1}1]$ direction of the GaAs(100) substrate, rotated by 90° compared with that in Au/Fe(6.0 nm)/GaAs from the same growth.[21] The origin of this uniaxial magnetic anisotropy might be related to the interface as that in the Fe/GaAs system. However, we would like to note that the origin of such uniaxial magnetic anisotropy in the Fe/GaAs(100) remains an open issue. Two distinctly different mechanisms associated with "unidirectional chemical bonding" and "magnetoelastic coupling," respectively, have been proposed to explain the uniaxial magnetic anisotropy in Fe/GaAs.[22,23] These two mechanisms might be responsible for the uniaxial magnetic anisotropy observed here. The anisotropy field as estimated from the saturation fields along the hard axes is around 300 Oe, greatly reduced compared with the high saturation field of about 1.6 kOe observed in Ref. 13. This might be due to a possible decrease of anti-phase boundaries in the epitaxial Fe_3O_4/GaAs structure.

The magnetic properties and the structure of the samples were further characterized using x-ray absorption spectroscopy (XAS) and XMCD, which are capable of probing the magnetic signal from sites of different chemical environments. Magnetite features an inverse spinel structure in which the tetrahedral sites are entirely occupied by Fe_{td}^{3+} cations but the octahedral sites are equally filled up by Fe_{oh}^{2+} and Fe_{oh}^{3+} cations. Although the same amount of Fe^{3+} cations in tetrahedral sites and octahedral sites are ferrimagneti-

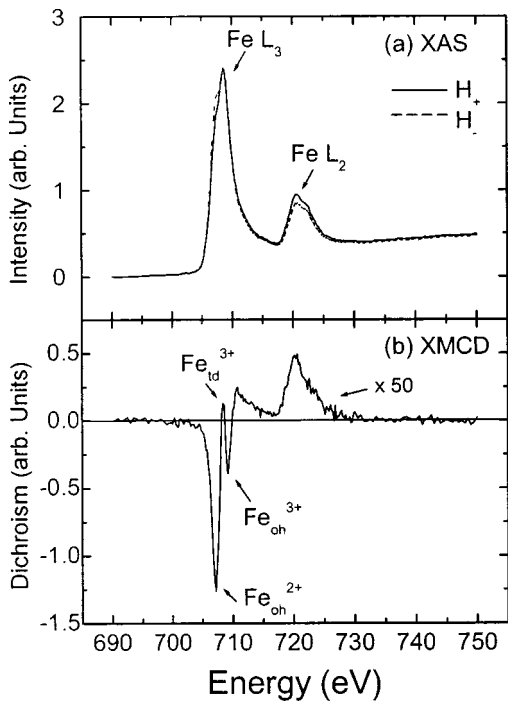FIG. 5. (a) XAS and (b) XMCD of Fe_3O_4 (6.0 nm)/GaAs(100). Three peaks in the Fe L_3 edge related to the Fe_{td}^{3+}, Fe_{oh}^{2+}, and Fe_{oh}^{3+} with different energy can be identified.

cally coupled, they can not cancel each other out in the dichroism due to their different chemical environments.[24] The measurements were carried out in station 1.1 in Daresbury in TEY mode. The 0.6 T magnetic field was parallel or antiparallel to the helicity of the incident x-ray, which was perpendicular or 45° with the surfaces of the measured films. Figure 5 shows the XAS and XMCD spectra from a 6.0 nm Fe_3O_4 sample with the x-ray perpendicular to the sample. For the 45° setup, the spectra were similar. The characteristic contributions from different sites of Fe_{td}^{3+}, Fe_{oh}^{2+}, and Fe_{oh}^{3+} in Fe_3O_4 can be clearly identified.[25] The strong peak of Fe_{oh}^{2+} also excludes the composition of γ-Fe_2O_3, which does not contain any Fe_{oh}^{2+}. The macroscopic magnetization comes from the octahedral Fe_{oh}^{2+} cations, which have different photon energies in the XMCD spectrum compared with the octahedral Fe_{oh}^{3+} cations or tetrahedral Fe_{td}^{3+} cations.

In summary, we have demonstrated the epitaxial growth of single-crystal Fe_3O_4 ultrathin films on GaAs(100) substrate by post growth annealing of ultrathin epitaxial Fe films in an oxygen partial pressure. The formation of the ferrimagnetic Fe_3O_4 rather than γ-Fe_2O_3 or other ion oxides has been confirmed by RHEED, XPS, and XMCD. The Fe_3O_4/GaAs(100) system shows an interesting epitaxial relationship with the unit cell of the Fe_3O_4 rotated by 45° to match that of GaAs(100) substrate. The Fe_3O_4 films show a uniaxial magnetic anisotropy, unexpected from the crystal symmetry, with the easy axis along the $[0\bar{1}1]$ direction of the GaAs(100) substrate. While the understanding of the fundamental structure and magnetism of this magnetic/semiconductor system remains challenging and will attract further experimental and theoretical studies, Fe_3O_4/GaAs(100) might be one of the most promising spintronic materials.

---

*Email address: yx2@ohm.york.ac.uk

[1] S.A. Chambers and Y.K. Yoo, MRS Bull. **28**, 706 (2003).

[2] J.M.D. Coey and C.L. Chien, MRS Bull. **28**, 720 (2003).

[3] S.A. Chambers and R.F.C. Farrow, MRS Bull. **28**, 729 (2003).

[4] B.T. Jonker, S.C. Erwin, A. Petrou, and A.G. Petukhov, MRS Bull. **28**, 740 (2003).

[5] A. Hirohata, Y.B. Xu, C.M. Guertler, J.A.C. Bland, and S.N. Holmes, Phys. Rev. B **63**, 104425 (2001).

[6] A.T. Hanbicki, B.T. Jonker, G. Itskos, G. Kioseoglou, and A. Petrou, Appl. Phys. Lett. **80**, 1240 (2002).

[7] H. Ohno, A. Shen, F. Matsukura, A. Oiwa, A. Endo, S. Katsumoto, and Y. Iye, Appl. Phys. Lett. **69**, 363 (1996).

[8] K.W. Edmonds, K.Y. Wang, R.P. Campion, A.C. Neuman, N.R.S. Farley, B.L. Gallagher, and C.T. Foxon, Appl. Phys. Lett. **81**, 4991 (2002).

[9] D. Chiba, K. Takamura, F. Matsukura, and H. Ohno, Appl. Phys. Lett. **82**, 3020 (2003).

[10] Y.S. Dedkov, U. Rudiger, and G. Guntherodt, Phys. Rev. B **65**, 064417 (2002).

[11] K.-i. Aoshima and S.X. Wang, J. Appl. Phys. **91**, 7146 (2002).

[12] F.C. Voogt, T.T.M. Palstra, L. Niesen, O.C. Rogojanu, M.A. James, and T. Hibma, Phys. Rev. B **57**, R8107 (1998).

[13] D.T. Margulies, F.T. Parker, F.E. Spada, R.S. Goldman, J. Li, R. Sinclair, and A.E. Berkowitz, Phys. Rev. B **53**, 9175 (1996).

[14] C. Ruby, J. Fusy, and J.-M.R. Genin, Thin Solid Films **352**, 22 (1999).

[15] W. Weiss and M. Ritter, Phys. Rev. B **59**, 5201 (1999).

[16] H.-J. Kim, J.-H. Park, and E. Vescovo, Phys. Rev. B **61**, 15 284 (2000).

[17] Y.B. Xu, E.T.M. Kernohan, D.J. Freeland, A. Ercole, M. Tselepi, and J.A.C. Bland, Phys. Rev. B **58**, 890 (1998).

[18] C. Ruby, B. Humbert, and J. Fusy, Surf. Interface Anal. **29**, 377 (2000).

[19] Y. Gao and S.A. Chambers, J. Cryst. Growth **174**, 446 (1997).

[20] T. Fujii, F.M.F. de Groot, G.A. Sawatzky, F.C. Voogt, T. Hibma, and K. Okada, Phys. Rev. B **59**, 3195 (1999).

[21] Here the easy axis of the uniaxial magnetic anisotropy is different with our previous result (Ref. 17).

[22] O. Thomas, Q. Shen, P. Schieffer, N. Tournerie, and B. Lepine, Phys. Rev. Lett. **90**, 017205 (2003).

[23] Y.B. Xu, D.J. Freeland, M. Tselepi, and J.A.C. Bland, Phys. Rev. B **62**, 1167 (2000).

[24] P. Kuiper, B.G. Searle, L.-G. Duda, R.M. Wolf, and P.J. van der Zaag, J. Electron Spectrosc. Relat. Phenom. **86**, 107 (1997).

[25] P. Morrall, F. Schedin, G.S. Case, M.F. Thomas, E. Dudzik, G. van der Laan, and G. Thornton, Phys. Rev. B **67**, 214408 (2003).